

Review

SiO₂@TiO₂ Composite Synthesis and Its Hydrophobic Applications: A Review

Alicia Rosales and Karen Esquivel * 

Graduate and Research Division, Engineering Faculty, Universidad Autónoma de Querétaro, Cerro de las Campanas, Santiago de Querétaro 76010, Mexico; alicia.ros.perez@hotmail.com

* Correspondence: karen.esquivel@uaq.mx; Tel.: +52-442-192-1200

Received: 14 December 2020; Accepted: 30 January 2020; Published: 2 February 2020



Abstract: Titanium dioxide is well known for its photocatalytic properties and low toxicity, meanwhile, silicone dioxide exhibits hydrophobic and hydrophilic properties and thermal stability. The union of these two materials offers a composite material with a wide range of applications that relate directly to the combined properties. The SiO₂-TiO₂ composite has been synthesized through physical methods and chemical methods and, with adequate conditions, morphology, crystallinity, boundaries between SiO₂-TiO₂, among other properties, can be controlled. Thus, the applications of this composite are wide for surface applications, being primarily used as powder or coating. However, the available research information on this kind of composite material is still novel, therefore research in this field is still needed in order to clarify all the physical and chemical properties of the material. This review aims to encompass the available methods of synthesis of SiO₂-TiO₂ composite with modifiers or dopants, the application and known chemical and physical properties in surfaces such as glass, mortar and textile, including aspects for the development of this material.

Keywords: SiO₂; TiO₂; composites; photocatalysis; hydrophobic

1. Introduction

The imitation of nature gives inspiration for the development of new technologies for pro-environmental remediation. Biomimetic is the term employed in the literature and in engineering for understanding the natural process for describing a perfect functional system where, over years of evolution, it yields the best adaptation to the environment [1]. In this kind of technology, we can find silicon oxide (SiO₂) and titanium dioxide (TiO₂). Both oxides are considered an example of biomimetic materials.

To give the biomimetic term to a material, a clear example of it needs to be presented. The “lotus effect” has extraordinary hydrophobic performance and self-cleaning features. With the rolling of water droplets, dust is removed from the surface with the movement of the water; in other words, it sweeps away contaminating particles. This phenomenon is called the self-cleaning property [2]. Hydrophobic and self-cleaning surfaces show great potential in industrial applications due to their morphology structure [3].

Many materials are inspired by nature, such as the structure of butterfly wings [4], the needle-shaped seta of water stride [5], gecko feed [6], and the morphology of the lotus leaf [7]. The lotus leaf has hierarchical micro and nanostructures on its surface. It is determined by a combination of surface chemistry and surface architecture [8]. Generally, the most hierarchical topography consists of multiple levels of roughness and micro and nanostructures on the surface [9]. It was observed that the lotus leaf was covered by about 10 μm sized protrusions at random with about 20 μm intervals among them, giving low-surface energy [10]. The surface architecture of hierarchically

rough surfaces reduces available contact area and the ability for water droplets to adhere to the surface. The measured contact angle is then a composite of the surface of air, as described by the Cassie-Baxter theory of wettability [11]. This is one of the classical models, and corresponding formulae about the surface wettability were established to understand the mechanism of hydrophobic phenomena from a theoretical perspective [12]. Based on these models, scientists not only theoretically explained the hydrophobic mechanism, but also calculated the contact angle (CA) of the corresponding surface [13].

The materials SiO₂ and TiO₂ have been used in separate ways, and have been widely reported in the literature with different synthesis methods and applications; however, the use of SiO₂-TiO₂ as a composite is reported in fewer papers. The lack of information about this kind of composite material limits the synthesis methods and applications. For that reason, more research in this field is needed in order to achieve a more complete review with all physical and chemical properties.

The review will focus on the hydrophobic surfaces of SiO₂ and TiO₂ with developments in synthesis methods, physicochemical properties, reaction mechanisms and applications in the fields of energy, environment, industry and others. The content is divided into three parts: a brief summary of basic theories including the hydrophobic phenomenon, self-cleaning properties in different surfaces (Section 2); Section 3 presents the methodologies for the synthesis of hydrophobic surfaces and their nanostructures and wettability. Practical applications of hydrophobic surfaces are shown in Section 4 such as in water self-cleaning, hydrophobic and anti-reflectivity. The last section summarizes the results and the challenges in the development of hydrophobic surfaces and the trends among this kind of surface.

2. Theory behind the Physico-Chemical Characteristics in SiO₂-TiO₂

Silicon dioxide (SiO₂) is a semiconductor compound with low toxicity, high thermal stability, and has both an amorphous and crystalline structure [14]. The properties have been extensively studied in different areas, such as electronics, photo-tonic, chemicals, environmental, electrochemistry, and biomedical fields [15–17]. The nobility of SiO₂ allows its union with different materials, such as TiO₂, one of the most studied photocatalysts. The SiO₂-TiO₂ composite provide the properties of both, where the SiO₂ is a support for the TiO₂ particles, with chemical, electronic and hydrophobic properties [18].

Self-cleaning is one of the most desired properties of the intelligent materials. This property is a typical phenomenon in nature; for thousands of years, natural evolution and selection has optimized functional systems, creating the ability of surfaces to repel contaminants such as solid particles and liquids. The first time this phenomenon was observed was in the leaves of the Lotus plant. Droplets of water deposited on the surface of the leaves maintained an almost perfect spherical shape, and rolled over the surface removing the particles of powder. Exhibiting not only a self-cleaning property but also extraordinary hydrophobic properties [2,19]. This phenomenon is called the “lotus effect” [20]. It is important to mention that this effect is not particular to the lotus plant, other plants and insects have hydrophobic surfaces [21]. For this reason, the lotus leaf only opened the doors for hydrophobic investigation.

In this context, the first studies in 1990 of hydrophobic surfaces discovered that some hydrophobic surfaces in nature exhibit other functional properties such as low wettability, antifogging, anti-reflection, and resistance [22]. Barthlott and Neinhuis et al. conducted the first research reporting the microstructure of the lotus leaf through scanning electron microscopy (SEM) [23]. Subsequently, Jian et al. found that a combination of multistructural micro and nanorugosity structures are fundamental for obtaining the self-cleaning phenomenon [24].

The presence of micro and nano structures on the surface provides low surface energy and surface tension, creating a rugosity in the surface, therefore obtaining a hydrophobic surface. Wettability is usually determined through the measurement of the contact angle of the water droplet on the surface. The contact angle is defined as the liquid-steam interface with respect to the solid-liquid interface. This angle is classified in three categories as shown in Figure 1 [25], hydrophilic surfaces exhibit

a contact angle of less than 90° ; hydrophobic surfaces present a contact angle higher than 90° and super hydrophobic surfaces present a contact angle higher than 150° .

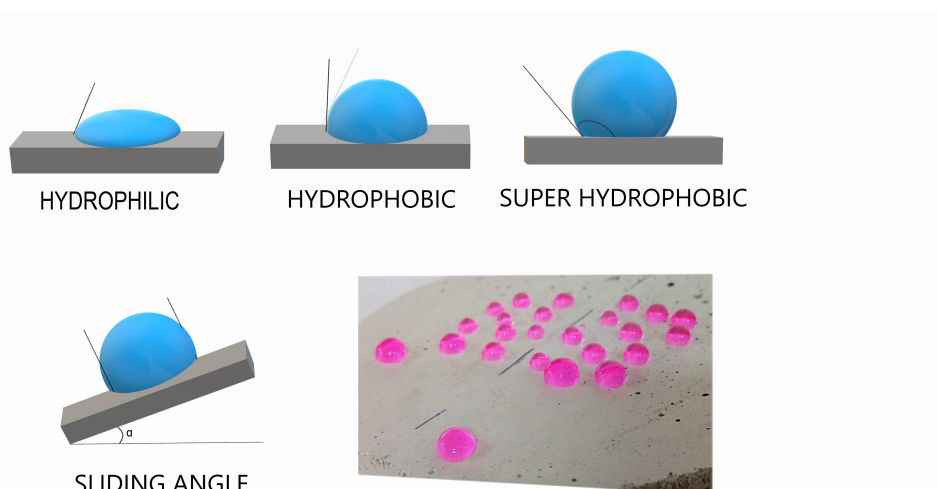


Figure 1. Contact angle and Sliding angle on the surface.

Thomas Young was the first person to describe the contact angle in 1805, established by the mechanical balance of the drop, acting with three interfacial tensions in an ideal solid surface [26]. Considering the contact angle is stable, it corresponds to a minimum of Gibbs free energy. Where Gibbs free energy states that the system must achieve a minimum of free energy when there is a liquid vapor balance. At constant temperature and pressure the surface tension is equal to Gibbs free energy per surface area [27,28]. The reduction of the surface's energy increases the hydrophobicity of the surface. Micro/nano surface texturing is another way to decrease the surface energy. In summary, the movement of the fluid over a solid surface can be achieved by two means, namely, the liquid follows the solid state, or it moves in the air trapped within the micro / nano texture on the surface [11].

Usually, self-cleaning surfaces need to be prepared in advance, namely, making a rough surface for low surface energy materials and chemically modifying the surface roughness to create a rough surface from low-surface energy materials. In this context, self-assembly organ silanes are one of the most employed strategies due to the high efficiency of making a surface hydrophobic by reducing surface energy [29].

The structure of the Polydimethyl Siloxane (PDMS) is a chain with an Si-O-Si structure and side chains of the $-\text{CH}_3$ groups. The structure exhibits thermal stability and elasticity, due to high bond energy and large bond angle. Furthermore, the $-\text{CH}_3$ groups have proportionate low surface energy and hydrophobicity as a result of the non-polar groups [30]. Moreover, PDMS with terminating methyl groups is hydrophobic silicone and can firmly adhere to the surface without using other additives. The hydroxyl groups of PDMS, which hydrolyzes during stirring, can interact with SiO_2 antiparticles by hydrogen bonding [31].

On the other hand, the Hexamethyldisilazane (HMDS) has methyl terminations, making it hydrophobic and making it an attractive material for creating a super hydrophobic surface and eliminating the need for complex chemical pathways [32]. HMDS forms the $(\text{CH}_3)_3\text{-Si-O}$ -group on Si wafer surfaces and on glass surfaces which changes these surfaces to lipophilic and indirectly facilitates the formation of a surface susceptible to the adhesion of organic impurities [33]. These modifiers of the surface enhance the self-cleaning properties. Moreover, compounds such as metallic oxides, ceramics or organic compounds offer different properties, such as photocatalytic activity. Among these compounds, TiO_2 is one of the materials with promising results.

TiO₂ is known for the diverse applications in different areas such as pharmaceutical, make up, environmental remediation, biomedical applications [34], devices and others [35]. Among the qualities of the material, low toxicity, chemical stability, and high availability stand out as advantages over other semiconductors. Also, due to these characteristics, TiO₂ is one of the most employed photocatalyst [36–38].

TiO₂ exhibits a high effectiveness in environmental remediation in the degradation of inorganic and organic pollutants. The photocatalytic properties are exhibited under irradiation with UV light, due to the band gap value of 3.2 eV, limiting the application. However, these properties can be increased by diminution of the band gap [39,40]. The photocatalytic process begins with the photogeneration of holes and electrons, which are diffusing to the surface, where reactive species react with the pollutant; as a result, a series of oxidation and reduction phenomena take place as shown in Figure 2 [41]. On the other hand, the physical properties of the TiO₂ such as morphology, surface area, crystalline phase and particle size of TiO₂, are well-known factors that directly impact on the photocatalysis mechanism [42,43].

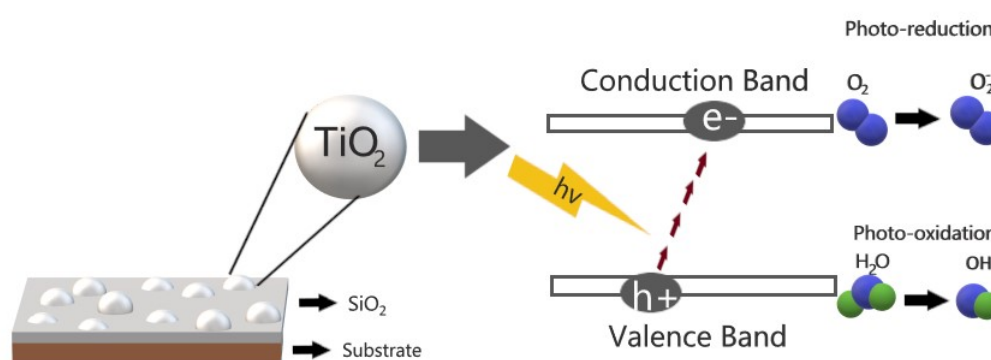


Figure 2. Photocatalytic activity of TiO₂ on SiO₂.

One of the main drawbacks that limits the use of TiO₂ is the method of application, since it is normally used in suspension. Typically, a loss of up to 30% of catalyst material is assessed for suspension applications [42]. For this reason, there is increasing interest in novel research in which TiO₂ is supported on a different material, SiO₂ has been employed as substrate for this purpose.

The union of SiO₂-TiO₂ has been achieved by different techniques such as sol-gel, impregnation, or precipitation [44]. In order to improve the yields of the desired reactions, the TiO₂ film must have certain characteristics such as well defined textural morphology and a proper thickness [45]. Moreover, the molar ratio of SiO₂-TiO₂ directly affects the crystallinity of the material, crystal size and porosity of the TiO₂. Furthermore, this material offers optical properties due to the high scattering of TiO₂ as a consequence of its large band gap and high refractive index. These properties allow the manufacture of antireflective and transparent surfaces of SiO₂-TiO₂ [46,47].

3. Synthesis Methods

Nanoparticles of TiO₂ and SiO₂ are found to have different structures. The methodologies employed yield different structural and physical properties.

3.1. Physical Methods

The physical methods are optimizable processes due to the precise conditions they use, such as high temperatures, pressures and high purity of precursors, which is why they are characterized by their high cost and limited applications.

3.1.1. Sputtering

Magnetron sputtering is a deposition technique involving a gaseous plasma which is generated and confined to a space containing the material to be deposited. First, pressure is stabilized typically in the mTorr range employing a pressure control system. After, the sputtering gas which is the plasma is flowed into the chamber. The surface of the sample is eroded by high-energy ions within the plasma, and the liberated atoms travel through the vacuum environment and deposit onto a substrate to form a thin film [48]. These collisions cause an electrostatic repulsion which 'knock off' electrons from the sputtering gas atoms, inducing ionization. The positive sputter gas atoms are now accelerated towards the negatively charged cathode, causing high energy collisions with the surface of the target [49]. In the interest of generating as many high energy collisions as possible, a high molecular weight gas such as argon or xenon is used as sputtering gas. The oxygen or nitrogen gases are employed for a reactive sputtering process [50]. Mezur et al. present the technique of magnetron sputtering with an additional microwave source to improve plasma ionization during deposition for the synthesis of TiO₂-SiO₂ thin films. The conditions of magnetron sputtering were of 10 kW DC power supply and 3 kW plasma source with Ti and Si targets with dimensions of 120 mm × 372 mm. The deposition rate of titania and silica was maintained at 1.1 Å/s oxygen and argon flow was equal to 56 sccm and 190 sccm, respectively. The microwave power was 2.7 kW, while power supplied to Ti and Si targets was 4 kW. The microwave plasma was activated for 5 min, providing additional cleaning of the substrates to remove organic residues. The results yield an anti-reflective, crack free coated surface, homogeneous and composed of small grains with maximum height of circa 7 nm to 12 nm [51].

Jeong et al. presents the deposition of dielectric films such as SiO₂ and TiO₂ at low substrate temperatures (<100 °C) by means of a sputtering technique. The process can be controlled with ease, which makes it a useful way to deposit high quality layers while maintaining good adhesion as well as coating uniformity [52]. The employed methodology of the sputtering technique involved the deposition of high purity (99.999% purity) ceramic targets of the materials (SiO₂ and TiO₂) on silicon wafers. The process was carried out in a high vacuum chamber (7×10⁻⁶ mbar) in the presence of different O₂/Ar+O₂ ratios. Further analysis of cross sectional transmission electron microscopy (TEM) images corroborated the variation of film structure towards a more dense and crystalline structure with the increase of temperature and also the presence of the anatase phase of TiO₂ [53].

3.1.2. Laser Ablation

Laser ablation is a combination of both vaporization and melt expulsion [54]. A focused beam of laser radiation strikes a surface, the electrons present in the substrate are excited by laser photons, the excitation results in generation of heat by absorption of photon energy. As consequence, the heating produces vaporization or fusion of the material. This transition results in the formation of a plasma plume. The initial heat generates a melt pool at the laser-substrate interaction zone. The temperature increases more with incoming pulses and the melt pool reaches the vaporization state, creating a high pressure, called recoil pressure, which pushes molten materials from the pool where they are ejected, increasing the temperature at the laser-substrate. The liquid reaches an explosive liquid-vapor phase transition stage, yielding geometric changes in the ablated features due to the resolidification of molten material [55,56].

Barberio et al. report that nanoparticles can be grown by laser ablation irradiated with the first harmonic of a Laser Nd:YAG (fluence of 500 mJ/cm², pulse of 7 ns and a frequency of 20 Hz) in solution. Obtaining TiO₂ and grains or wafer of SiO₂. The shape and dimensions of the produced nanoparticles were controlled measuring the optical absorption of the solution during the irradiation. Atomic force microscopy (AFM) and scanning electron microscopy (SEM) images confirm the presence of particles with an average size of 9.82 nm and 14.83 nm for SiO₂ and TiO₂ nanoparticles, respectively, and very low standard deviations (in the range of 0.02–0.04 nm for both particles species). Also, this layer is perfectly transparent, uniform, and hydrophobic [57].

3.2. Chemical Methods

Chemical methods are processes that produce a chemical compound from a chemical precursor. The SiO₂-TiO₂ compound is mainly obtained by chemical synthesis.

3.2.1. Sol-Gel

Sol-gel reactions have been extensively studied as a method to prepare organic, inorganic and ceramics compounds, at low temperature and pressure [58]. The process is divided into two reactions; hydrolysis and condensation. The hydrolysis replaces alkoxide groups with hydroxyl groups, generally catalyzed by the presence of an acidic or alkaline medium. During the hydrolysis and condensation reactions, secondary products of low-molecular-weight as ethanol and water molecules are generated. These molecules must be removed from the solutions [59,60]. Much research has focused on synthesizing ceramic compounds such as TiO₂ and SiO₂ independently by the sol-gel method as well as TiO₂-SiO₂ composites due to its low cost, operation conditions and single step doping in situ.

Son et al. fabricated SiO₂/TiO₂ core shell nanoparticles to investigate the influence of the size and refractive index of light-scattering particles on light-scattering properties [61,62]. On the other hand, Lee et al. synthesized SiO₂/TiO₂ core shell particles with variable shell thickness by a multistep sol-gel coating process. Titania coating on the silica particles increased the electrophoretic mobility and the specific surface area increased depending on the number of coating steps, attributed to the textured titania coating layer [63].

The feasibility of the sol-gel method allows the modification of the synthesis of the SiO₂-TiO₂ composite by adding modifiers and dopants that enhance its properties. Ang et al. prepared a series of nitrogen-doped TiO₂-SiO₂ were prepared by a sol-gel method through varying the TiO₂/SiO₂ molar ratio, employed TTIP and TEOS as precursors of TiO₂ and SiO₂ respectively. The results showed photocatalytic activity was modified for structural and morphology properties such as, amount of SiO₂ on the surface, TiO₂ particle size, surface area of TiO₂, and the formation of Brønsted acid sites on the surface [64]. On the other hand, Kim et al. reports the synthesis of a nitrogen doped SiO₂/TiO₂ core shell by the sol-gel method in a stepwise manner, obtaining a completely encapsulated SiO₂ nanoparticle by the TiO₂ shell with uniform size distribution and enhanced photocatalytic activity [65]. Finally, Den et al. report a simple and practical approach to the facile production of TiO₂-SiO₂@PDMS - HDMS versatile hybrid films via a sol-gel process. Obtained by hydrolyzing TEOS in the presence of acetic acid and anhydrous ethanol, and a constant temperature of 70 °C for 20 h in a closed container [66].

Kitsou et al. presented the synthesis of SiO₂@TiO₂ core shell nanoparticles modified with hyperbranched poly(ethyleneimine) (HBPEI). HBPEI was added as dispersant to form a thick homogeneous shell of nanostructure. The suspension was kept under magnetic stirring for 24 h to remove the excess of precursor. Obtaining a shell constituted of pure anatase particles of 7 nm in diameter in comparison with pure TiO₂, which yields greater particles between 15 and 30 nm and a mixture of anatase and rutile phases. As a consequence, there was an increment of 2.5 times in the surface area [67].

Kapridaki et al. present the design and synthesis of a SiO₂-TiO₂ coating with PDMS for potential application in monument conservation due to its optical and hydrophobic properties. An analysis of X-ray diffraction (XRD) presents the existence of an anatase phase of TiO₂, with a crystallite size of 5 nm [68]. Continuing with the investigation, Kapridaki et al. studied different concentrations of oxalic acid. The study exhibits the high importance of oxalic acid as a catalyst during the synthesis, a crack-free agent over application and a hole-scavenger over photocatalytic properties [69]. On the other hand, Jiameje et al. studied the variation of amounts of PDMS over the SiO₂-TiO₂ coating and found that the gelation time decreased as the amount of PDMS increased [70]. Furthermore, over processing of condensation of the PDMS facilitates the increase in the degree of cross and consequence? a major flexibility [24].

3.2.2. Sonochemistry Coupled Sol-Gel

Sonochemistry is a new technique in the process of polymerization, catalytic chemistry reaction, synthesis of materials and synthesis of inorganic nanostructure with applications in science and technology [71,72]. This technique is called “green chemistry”, for the short times of reactions [73]. Sonochemistry is a process of acoustic cavitation involving the fast growing and collapse of the microbubbles in liquid media in a very short period, generating hot spots with temperatures and pressure of around 5000 K and 1000 bar, respectively, with a collapse velocity of around -1360 m/s [74,75]. The principal reaction occurs inside the bubble. Due to these extreme conditions organic molecules could be destroyed directly or decomposed with radicals ($^{\cdot}\text{O}_3\text{H}$ -, $^{\cdot}\text{O}_2$, OH_2 , etc.) formed during the collapse of the microbubble. In new research, the use of sonochemistry makes a difference in reaction times and exhibits different structural properties [62,71]. Rosales et al. coupled the sol-gel method with sonochemistry for the synthesis of a $\text{SiO}_2@\text{TiO}_2$ coating. The aim was to reduce the synthesis time of conventional sol-gel compared to a sonochemistry coupled method. It was proven that the sonochemistry energy was enough for the crystallization of the anatase phase of TiO_2 given the photocatalytic properties and the preparation of nano and micro roughness for hydrophobic properties, with the amorphous phase of SiO_2 [76].

3.2.3. Hydrothermal

Hydrothermal methods are an important branch of inorganic synthesis. We et al. describes the hydrothermal synthesis of new materials including single crystals, microporous, complex oxides, and inorganic-organic hybrid materials [77]. Grover et al. report a simple method of synthesizing titanium dioxide nano rods via a hydrothermal route using P25 TiO_2 as a precursor, obtained TiO_2 nanorods were calcined at 500 °C. SiO_2 - TiO_2 composite was prepared by mixing the previously obtained TiO_2 , SiO_2 precursor with ethanol, and concentrated H_2SO_4 . The system was refluxed at 80 – 90 °C for 1 h. The results show a large difference in the surface area, showing major catalytic activity in the degradation of contaminants such as naphthalene and anthracene with respect to other catalysts [78]. On the other hand, Zhang et al. present the synthesis of $\text{SiO}_2@\text{TiO}_2$ hybrid nanoparticles by a solvothermal method employing tetrabutyl titanate ($\text{Ti}(\text{O}i\text{Bu})_4$) as a precursor of TiO_2 . As a result, the $\text{SiO}_2@\text{TiO}_2$ hybrid nanoparticles, presented a core diameter of 437 nm and shell thickness of 50 nm. The XRD analysis confirm the presence of anatase phase of TiO_2 in the shell structure [79]

3.2.4. Chemical Vapor Deposition

Chemical Vapor Demosition (CVD) is currently used for depositing a wide variety of films on the float glass process in solid thin films. Obtaining a large density, good stoichiometry and uniformity over a large area. One of the main drawbacks of this method is that it requires a high temperature to produce high quality materials, and the substrate cannot tolerate being heated [80]. Nevertheless, it does not require as high a vacuum as some other processing methods, and films can be favorably deposited even at atmospheric pressure. The description of the deposition of SiO_2 - TiO_2 using CVD has rarely been reported. Lee et al. describe the deposition behavior of SiO_2 - TiO_2 thin films, using CVD processing and volatile alkoxide precursors. It was found that the process of deposition of SiO_2 and TiO_2 are not the same, due to disposition of the alkoxide radicals. Furthermore, the refractive indices of SiO_2 - TiO_2 thin films were determined with values of 1.5 and 2.3, respectively [81].

A summary of different synthesis methods of SiO_2 - TiO_2 composites are shown in Table 1. It is possible to observe that physical and chemical methods differ in equipment and synthesis conditions, note that physical methods requires sophisticated equipment with rigorous control on conditions. Furthermore, the resulting morphology and structure of the SiO_2 - TiO_2 composite can be tuned easily by applying chemical methods rather than the physical methods which have been used mostly for layer deposition [82]. Methods such as sputtering and laser ablation allow the control of the crystallite size, crystalline phase, uniform and thickness of layer of the SiO_2 - TiO_2

composite, such as Barberio et al.'s work on growing nanoparticles of TiO_2 with SiO_2 , controlling size, with a low deviation. On the other hand, the chemical methods are more frequently employed due to less sophisticated equipment and variable conditions of synthesis, which yields different properties of the material such as photocatalytic, hydrophobic, high porosity, and antireflectant. These methods allow the control of the size of the crystal, morphology, structure and dopants or modifiers such as PDMS [83], HDMS [84], nitrogen [85], among others. Work such as that by as Kapridaki et al. and Wu et al. synthesized the SiO_2 - TiO_2 employing the sol-gel methodology with different conditions, obtaining different morphology, properties and applications.

The different tunable morphology obtained through the different synthesis methods yields materials with specific physicochemical properties, which can be useful for a particular application. Figure 3 shows some of the different morphology that can be obtained through the physical and chemical synthesis methods, particularly, the core-shell morphology is better controlled through the sol-gel method. However, the versatility of the method allows the obtaining of other morphologies such as raspberry or nanoparticles. Nevertheless, the sol-gel method is not the only option as these morphologies can be achieved through hydrothermal synthesis or sonochemical synthesis. On the other hand, physical methods such as laser ablation are one of the better options when synthesizing thin films, given the sensibility of the technique that allows better thickness control and particle size.

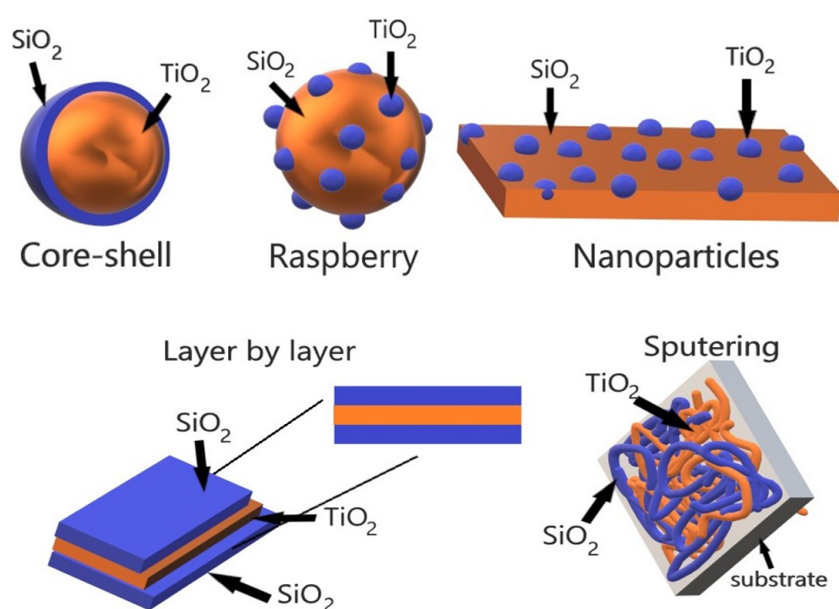


Figure 3. Morphology of the TiO_2 - SiO_2 composite.

Table 1. Methods and synthesis of the Si_2 - TiO_2 composite.

Method	Conditions	Morphology	Crystallite (nm)	Reference
Layer by layer	550 °C, 10 h, 1 atm	Thin film	3.5–8.4	[86]
Laser Ablation	Fluence of 500 mJ/cm^2 , pulse of 7 ns, Frequency of 20 Hz	Nanoparticles	9–15	[57]
Hydrothermal	200–800 °C, 1 h, reflux	Core-Shell	60	[78]
Hydrothermal	500 °C, 36 h	Spheres	50	[79]
Sol-gel	Centrifuged, 24 h	Raspberry	7.9	[87]
Hetero-coagulation	Centrifugation	Spheres	10	[88]
Sol-gel	550 °C, 14 h	Core-Shell	95	[89]
Hydrolysis	350 °C, 8 h	Spheres	30	[90]
Sol-gel	Magnetic stirring, 25 h	Nanoparticles	5	[69]
Sputtering	10 kW DC, 3 kW Plasma sour	Nanoparticles	7	[51]
Sonochemistry	30 min, High temperature	Nanoparticles	14	[76]

4. Applications

4.1. Hydrophobicity

Kapridaki et al. reported the application of a SiO₂-TiO₂ hybrid coating on marble surfaces. The marble hydrophobicity enhancement was presented with a 34% decrease of the water vapor permeability and a reduction of the water capillary coefficient. As a consequence, a notable increment of the contact angle in the treated surfaces was observed. The application of the coating on the marbles surfaces was carried out by brushing. The contact angle showed a diminution of 1–2° after 20 min of UV-Vis irradiation [68]. On the other hand, Wu et al. reported an antireflection coating of modified SiO₂@TiO₂ on glass substrates fabricated by using a dip-coating machine. The glass substrates was coated with urb-hSiO₂@TiO₂, after the coating was dried, a calcination process was carried out at 550 °C for 2 h. The initial CA was 107.9°. Afterward, the coated glass substrates were irradiated with UV light. Results show that with a short time of irradiation the CA was rapidly decreased. After 8.5 h of irradiation the final CA was 0°. This effect is attributed to the photocatalytic properties of TiO₂. Furthermore, the decrease of the CA is attributed to the degradation of the surface hydrophobic alkyl chain [87]. Moreover, Mezur et al. determined the wettability of the antireflection SiO₂-TiO₂ coating, based on the contact angle measurement. The CA was equal to 91.1° and a roughness lower of 1.4 nm [51].

4.2. Antireflective Properties

Zhang et al. created a double-layered TiO₂-SiO₂ nanostructure film with self-cleaning and antireflection properties. The films were prepared layer-by-layer employing different routes of synthesis. The results demonstrated that the combined properties of self cleaning and antireflection could be created in double-layered TiO₂-SiO₂ nanostructured films [91]. Previously, Miao et al. prepared a SiO₂-TiO₂ coatings by depositing double-layers onto glass substrates using a combined sol-gel dip-coating process in which the two oxide layers were deposited in succession [92]. On the other hand, Ye et al. designed a material of triple-layer broadband abrasion-resistant and antireflective (AR), employing SiO₂, TiO₂ and SiO₂-TiO₂ hybrid. Synthesized through the sol-gel method using TBOT and TEOS as precursors, and employing HDMS to modify the surface of the AR coatings. The results showed an average transmittance of 98.4% in the visible region and CA variation in the function of HMDS concentration [93].

Mazur et al. prepared and studied an antireflection multilayer coating, employing a combination of five TiO₂ and SiO₂ thin films on glass substrates. The results showed amorphous structures with low surface roughness. The transmittance in the visible wavelength range was increased after the deposition of the AR coating as-compared to glass substrate, obtaining transmittances above 97% in the visible spectrum range with as low a number of layers as possible. Furthermore, the TiO₂ layer on the top is narrower with a thickness of 10 nm, with the purpose of maintaining the high transparency [51]. The recent research of Wu et al. reported that the modification of the SiO₂@TiO₂ coating with an organic chemical compound and under the optimal conditions. The results showed an increase of the average transmittance and refractive index of 99.04% and 1.218, respectively, in the range of 400–800 nm, presenting an excellent antireflection performance [87].

4.3. Anti-Fogging

Tricoli et al. synthesized nanofibers of SiO₂ and nanoparticles of TiO₂ were deposited onto glass substrates by flame spray pyrolysis of organometallic solutions and stabilized by in situ flame annealing, finding that the minimal thickness of 200–300 nm of as deposited coatings or films was necessary to obtain full anti-fogging performance. The in situ annealed coatings preserved their super-hydrophilicity and anti-fogging functionality after being flushed with water [94]. Miyauchi et al. fabricated thin films of TiO₂/SiO₂/WO₃, which exhibited excellent sustainability of the anti-fogging property even in indoor conditions, attributing this property the effect

of photocatalytic oxidation activity and photoinduced hydrophilicity of TiO₂ and the hydrophilic property of SiO₂ [95]. Eshaghi et al. researched the thin film of SiO₂/TiO₂/SiO₂ deposited on glass substrates using an electron beam physical vapor deposition technique. The SiO₂/TiO₂/SiO₂ film showed higher transmittance and a lower refractive index in comparison to SiO₂/TiO₂ thin film. They demonstrated that by covering TiO₂ thin film with a SiO₂ over layer the hydrophilicity was significantly improved and an anti-fogging effect was obtained. Therefore, they suggest that SiO₂/TiO₂/SiO₂ thin film would be very useful where super-hydrophilicity and an anti-fogging effect are desired for automobile and optical lens applications [96].

4.4. Photocatalytic Activity

Degg et al. determined the photocatalytic activity of the TiO₂-SiO₂@PDMS hybrid powder by testing the degradation of the methylene blue colorant, measured in a dyed film and in dyed water solution, both under UV irradiation (365 nm). The discoloration was completed within 30 min, with a minor decrease in the CA of 5–6° [66]. On the other hand Tang et al. used the sol-gel method to prepare nano-SiO₂-TiO₂ composite fiber and found that the product exhibited the highest photocatalytic activity when the calcination temperature was 800 °C [97]. Liu et al. used the electrospinning method to prepare nano-SiO₂-TiO₂ composite fiber, presenting high photocatalytic activity [98].

L. Wu et al. used a gaseous detonation method to prepare a composite of SiO₂-TiO₂. The presence of SiO₂ inhibited the growth of TiO₂ particles and the transformation from anatase phase into rutile phase. As a consequence of the thin and uniform amorphous SiO₂ layers, that was covering the surface of TiO₂ particles, inhibiting the growth of the particles and phase change of them. Furthermore, the high presence of amorphous SiO₂ layers obstruct the redox reaction between electrons and holes on the surface of the TiO₂ particles, diminishing the photocatalytic activity of the particle, and therefore the time of degradation of the colorant. Nonetheless, samples with content 5% mol of SiO₂ present anatase phase structure TiO₂ particles with an optimal photocatalytic activity, with an average particle size of 15.3 nm and a specific surface area of 77 m²/g [99].

Resende et al. prepared a composite of SiO₂-TiO₂ particles with low molar ratio between them, synthesized through a hydrothermal method with a calcination of under 800 °C, the TiO₂ particles showed an anatase-phase structure and high specific surface [100]. On the other hand, Dong et al. prepared SiO₂-TiO₂ nanocomposite with anatase phase of TiO₂ nanocrystals and amorphous SiO₂ nanoparticles, characteristics for mesoporous structure and high specific surface area and high photocatalytic activity with a stable repeatability [101]. Kitsou et al. present an optimum core-shell nanoparticles material that showed a better performance than that of pure titania, that is, 89.71% vs. 88.54% degradation percentage and a higher degradation rate (0.62 vs 0.55 lmicrog/m²s) [67,102].

4.5. Textile Application

Yuranova et al. investigated the photocatalytic activity of TiO₂-SiO₂ coating over cotton textiles, colored with red wine. The cotton fibers were dip-coated with the mixed colloids of TiO₂ and SiO₂. Afterward, a thermal treatment was carried out with the purpose of obtaining high dispersed TiO₂ particles surrounded by amorphous SiO₂. Results showed a better efficiency of TiO₂-SiO₂-coated cotton samples than TiO₂-coated cotton samples [103]. Moreover, Fakin et al. synthesized and characterized nanoparticles of TiO₂-SiO₂, with the purpose of being utilized in functional dyeing as combined reactive dyeing of cotton fabrics [104]. On the other hand, Veronoski et al. synthesized nanoparticles of TiO₂ and applied them to man-made cellulose fibers, which facilitates the photocatalysis activity [105]. Pakdel et al. functionalized wool fabrics using TiO₂/SiO₂ nanocomposites through a low-temperature sol-gel method. The self-cleaning and hydrophilicity properties were evaluated in wool fabrics through the removal of coffee stains under UV irradiation [106]. Carrying on with the research led to the functionalization of cotton fabrics with TiO₂/SiO₂, yielding a synergistic function with the SiO₂ with the properties of TiO₂ [107].

Other research modified the composite with organic chemical compounds or inorganic compounds. Deng et al. obtained a TiO₂–SiO₂ suspension with PDMS, which was applied to a polyester-cotton fabric with the purpose of obtaining flexibility, low-toxicity and a high contact angle in the coating. Results showed the initial CA was 158° and the SA was 4°. Afterward, the coated fabrics were tested to determine the washing durability and abrasion resistance; the diminution of the CA was of 10°. Finally, after being attacked by strong basic the CA diminution was 32° less. However, the analysis of TEM did not show morphology change [66]. Xu et al. prepared a coating of SiO₂–TiO₂ modified with Methyltrimethoxysilane (MTMS). The cotton fabrics coated with the TiO₂–SiO₂ composite particles exhibit simultaneous superhydrophobicity and a photocatalytic self-cleaning property [108]. Landi et al. studied the photocatalytic ability of SiO₂–TiO₂ and SiO₂–TiO₂–HY (zeolite) coated textile substrates. Photocatalytic activity was evaluated by monitoring, over time, the degradation of Rhodamine B dye (RhB), a typical textile industry pollutant [109].

The properties and applications of the TiO₂–SiO₂ composite are shown in Table 2. It is possible to observe that one of the most exploited properties of the TiO₂–SiO₂ composite is the photocatalytic property, regardless of the substrate, namely, mortar, marbel, glass, or suspension due to the flexibility to adapt with the SiO₂ [110]. The TiO₂–SiO₂ composite with photocatalytic properties present other properties such as antireflective and hydrophobic, the latter is normally complicated to achieve due to the nature of TiO₂ [111]. Authors such as Deeg et al. and Deng et al. tested the photocatalytic activity under UV-Vis irradiation, keeping a high contact angle modifying the TiO₂–SiO₂ composite with PDMS. On the other hand, the high antireflective and hydrophobic properties are usually desired for glass substrates [112]. Ye et al. obtained a material with a transmittance of 98.4% and hydrophobic, by modifying the TiO₂–SiO₂ composite with HDMS. In the case of textile fibers, properties such as photocatalytic, hydrophobic and abrasion resistance are wanted for research, such as that by Pakdel et al. and Veronoski et al.

Table 2. Properties of the SiO₂–TiO₂ composite.

Substrate	Properties	Contact Angle	Photocatalytic Activity	Reference
Glass	Hydrophilic, Anti-reflective, Transparent Anti-fogging	16.7–10.6 °C	–	[86]
Suspension	Photocatalytic	–	73%	[78]
Suspension	Photocatalytic	–	66%	[79]
Glass	Hydrophobic Transmittance	107°	–	[87]
Suspension	Self-cleaning	–	10%	[88]
Mortar	Photocatalytic	–	100%	[89]
Glass	Transmittance, Self-cleaning, photocatalytic	31–34°	–	[90]
Mortar, Glass	Transmittance, self-cleaning	97°	70.5%	[76]
Marbel	Hydrophobic, Photocatalytic	104°	–	[69]
Cotton fabrics	Hydrophobic, Photocatalytic	160.5°	–	[108]

5. Conclusions

The diversity of physical and chemical synthesis methodologies allow us to obtain different morphologies, crystalline phases, and properties. Chemical methods offer a greater flexibility of synthesis with less stringent conditions. However, physical methods offer a control over thickness and uniformity layer by layer. TiO₂ and SiO₂ are typical optical thin films that exhibit high transparency and low absorption in the visible and near infrared wavelength range, but with a different reflection index.

Although SiO₂ does not exhibit photocatalytic properties, its high porosity and large specific surface area makes it suitable as an adsorbent. As a consequence, an increase of reactant concentration on the TiO₂ surface can be assessed, improving the photocatalytic activity of TiO₂. Moreover, the presence of SiO₂ has a positive effect on the enlargement of TiO₂ specific surface area. It also inhibits the phase change and grain growth of TiO₂ and, overall, it contributes to the enhancement of the photocatalytic activity of TiO₂, confirming the synergistic role of silica in this type of composite and in different substrates.

The hydrophobic properties of the composite SiO₂-TiO₂ are of great interest for researchers in the field, however, the contribution of TiO₂ decreases these properties, yielding a low contact angle. Nevertheless, the addition of different compounds, such as PDMS or HDMS have proven to increase the contact angle and therefore the hydrophobic properties.

The applications of the SiO₂-TiO₂ composite over different surfaces with notable roughness between substrates, such as textiles, mortar, glass or marble, is made possible due to the methods of synthesis, which offer different conditions of synthesis and allow us to add additives that chemically modify the surface and improve the properties of interest thus making it a tunable composite with a wide variety of applications.

Author Contributions: Conceptualization, Writing—Review and Editing, K.E.; Writing—Original Draft Preparation, A.R. All authors have read and agreed to the published version of the manuscript.

Funding: FOFI-UAQ-2018.

Acknowledgments: CONAcYT for scholar ship granted and to the FOFI-UAQ 2018 for the financial support.

Conflicts of Interest: The authors declare no conflict of interest.

Abbreviations

The following abbreviations are used in this manuscript:

TiO ₂	Titanium dioxide
SiO ₂	Silicon dioxide
TEOS	Tetraethyl orthosilicate
EtOH	Ethanol
CO ₂	Dioxide carbon
H ₂ SO ₄	Sulfuric acid
PDMS	Polydimethyl siloxane
HMDS	Hexamethyldisiloxane
HBPEI	Poly(ethyleneimine)
MTMS	Methyltrimethoxysilane
(Ti(OBu) ₄)	Tetrabutyl titanate
H ₂ O	Water destilate
TTIP	Titanium tetraisopropoxide
RhB	Rhodamine B
XRD	Diffraction X-Ray
SEM	Scanning Electron Microscopy
AFM	Atomic Force Microscopy
CVD	Chemical Vapor Deposition
CA	Contact Angle
SA	Sliding Angle

References

1. Elbourne, A.; Crawford, R.J.; Ivanova, E.P. Nano-structured antimicrobial surfaces: From nature to synthetic analogues. *J. Colloid Interface Sci.* **2017**, *508*, 603–616. [[CrossRef](#)] [[PubMed](#)]
2. Cheng, Y.T.; Rodak, D.E. Is the lotus leaf superhydrophobic? *Appl. Phys. Lett.* **2005**, *86*, 144101. [[CrossRef](#)]
3. Neinhuis, C.; Barthlott, W. Characterization and distribution of water-repellent, self-cleaning plant surfaces. *Ann. Bot.* **1997**, *79*, 667–677. [[CrossRef](#)]
4. Sun, M.; Watson, G.S.; Zheng, Y.; Watson, J.A.; Liang, A. Wetting properties on nanostructured surfaces of cicada wings. *J. Exp. Biol.* **2009**, *212*, 3148–3155. [[CrossRef](#)]
5. Hasan, J.; Webb, H.K.; Truong, V.K.; Watson, G.S.; Watson, J.A.; Tobin, M.J.; Gervinskis, G.; Juodkazis, S.; Wang, J.Y.; Crawford, R.J.; et al. Spatial variations and temporal metastability of the self-cleaning and superhydrophobic properties of damselfly wings. *Langmuir* **2012**, *28*, 17404–17409. [[CrossRef](#)]

6. Eduok, U.; Szpunar, J. Bioinspired and hydrophobic alkyl-silanized protective polymer coating for Mg alloy. *Prog. Nat. Sci. Mater. Int.* **2018**, *28*, 354–362. [[CrossRef](#)]
7. Liu, K.; Yao, X.; Jiang, L. Recent developments in bio-inspired special wettability. *Chem. Soc. Rev.* **2010**, *39*, 3240–3255. [[CrossRef](#)]
8. Wang, J.; Chen, H.; Sui, T.; Li, A.; Chen, D. Investigation on hydrophobicity of lotus leaf: Experiment and theory. *Plant Sci.* **2009**, *176*, 687–695. [[CrossRef](#)]
9. Cheng, Y.T.; Rodak, D.; Wong, C.; Hayden, C. Effects of micro-and nano-structures on the self-cleaning behaviour of lotus leaves. *Nanotechnology* **2006**, *17*, 1359. [[CrossRef](#)]
10. Shirtcliffe, N.J.; McHale, G.; Atherton, S.; Newton, M.I. An introduction to superhydrophobicity. *Adv. Colloid Interface Sci.* **2010**, *161*, 124–138. [[CrossRef](#)]
11. Giacomello, A.; Meloni, S.; Chinappi, M.; Casciola, C.M. Cassie–Baxter and Wenzel states on a nanostructured surface: Phase diagram, metastabilities, and transition mechanism by atomistic free energy calculations. *Langmuir* **2012**, *28*, 10764–10772. [[CrossRef](#)] [[PubMed](#)]
12. Forsberg, P.; Nikolajeff, F.; Karlsson, M. Cassie–Wenzel and Wenzel–Cassie transitions on immersed superhydrophobic surfaces under hydrostatic pressure. *Soft Matter* **2011**, *7*, 104–109. [[CrossRef](#)]
13. Wang, G.; Guo, Z.; Liu, W. Interfacial effects of superhydrophobic plant surfaces: A review. *J. Bionic Eng.* **2014**, *11*, 325–345. [[CrossRef](#)]
14. Pacchioni, G.; Skuja, L.; Griscom, D.L. *Defects in SiO₂ and Related Dielectrics: Science and Technology*; Springer Science & Business Media: Berlin, Germany, 2012; Volume 2.
15. Li, C.; Ma, C.; Wang, F.; Xi, Z.; Wang, Z.; Deng, Y.; He, N. Preparation and biomedical applications of core–shell silica/magnetic nanoparticle composites. *J. Nanosci. Nanotechnol.* **2012**, *12*, 2964–2972. [[CrossRef](#)] [[PubMed](#)]
16. Nandanwar, R.; Singh, P.; Haque, F.Z. Synthesis and characterization of SiO₂ nanoparticles by sol-gel process and its degradation of methylene blue. *Am. Chem. Sci. J* **2015**, *5*, 1–10. [[CrossRef](#)]
17. Hosseini, S.; Ahmadi, Z.; Nemati, M.; Parvizian, F.; Madaeni, S. Electrodialysis heterogeneous ion exchange membranes modified by SiO₂ nanoparticles: fabrication and electrochemical characterization. *Water Sci. Technol.* **2016**, *73*, 2074–2084. [[CrossRef](#)]
18. Wu, Z.; Lee, D.; Rubner, M.F.; Cohen, R.E. Structural color in porous, superhydrophilic, and self-cleaning SiO₂/TiO₂ Bragg stacks. *Small* **2007**, *3*, 1445–1451. [[CrossRef](#)]
19. Frankiewicz, C.; Zoueshtiagh, F.; Talbi, A.; Streque, J.; Pernod, P.; Merlen, A. From ‘petal effect’ to ‘lotus effect’ on the highly flexible Silastic S elastomer microstructured using a fluorine based reactive ion etching process. *J. Micromech. Microeng.* **2014**, *24*, 115008. [[CrossRef](#)]
20. Zhang, M.; Feng, S.; Wang, L.; Zheng, Y. Lotus effect in wetting and self-cleaning. *Biotribology* **2016**, *5*, 31–43. [[CrossRef](#)]
21. Fang, Y.; Sun, G.; Bi, Y.; Zhi, H. Multiple-dimensional micro/nano structural models for hydrophobicity of butterfly wing surfaces and coupling mechanism. *Sci. Bull.* **2015**, *60*, 256–263. [[CrossRef](#)]
22. Faustini, M.; Nicole, L.; Boissiere, C.; Innocenzi, P.; Sanchez, C.; Grosso, D. Hydrophobic, antireflective, self-cleaning, and antifogging sol-gel coatings: An example of multifunctional nanostructured materials for photovoltaic cells. *Chem. Mater.* **2010**, *22*, 4406–4413. [[CrossRef](#)]
23. Barthlott, W.; Neinhuis, C. Purity of the sacred lotus, or escape from contamination in biological surfaces. *Planta* **1997**, *202*, 1–8. [[CrossRef](#)]
24. Stanton, M.M.; Ducker, R.E.; MacDonald, J.C.; Lambert, C.R.; McGimpsey, W.G. Super-hydrophobic, highly adhesive, polydimethylsiloxane (PDMS) surfaces. *J. Colloid Interface Sci.* **2012**, *367*, 502–508. [[CrossRef](#)] [[PubMed](#)]
25. Kwok, D.Y.; Neumann, A.W. Contact angle measurement and contact angle interpretation. *Adv. Colloid Interface Sci.* **1999**, *81*, 167–249. [[CrossRef](#)]
26. Marmur, A. Wetting on hydrophobic rough surfaces: To be heterogeneous or not to be? *Langmuir* **2003**, *19*, 8343–8348. [[CrossRef](#)]
27. Nishino, T.; Meguro, M.; Nakamae, K.; Matsushita, M.; Ueda, Y. The lowest surface free energy based on-CF₃ alignment. *Langmuir* **1999**, *15*, 4321–4323. [[CrossRef](#)]
28. Meiron, T.S.; Marmur, A.; Saguy, I.S. Contact angle measurement on rough surfaces. *J. Colloid Interface Sci.* **2004**, *274*, 637–644. [[CrossRef](#)]

29. Murashkevich, A.; Alisienok, O.; Zharskii, I. Physicochemical and photocatalytic properties of nanosized titanium dioxide deposited on silicon dioxide microspheres. *Kinet. Catal.* **2011**, *52*, 809–816. [[CrossRef](#)]
30. Cui, X.; Zhu, G.; Pan, Y.; Shao, Q.; Dong, M.; Zhang, Y.; Guo, Z. Polydimethylsiloxane-titania nanocomposite coating: fabrication and corrosion resistance. *Polymer* **2018**, *138*, 203–210. [[CrossRef](#)]
31. Zárraga, R.; Cervantes, J.; Salazar-Hernandez, C.; Wheeler, G. Effect of the addition of hydroxyl-terminated polydimethylsiloxane to TEOS-based stone consolidants. *J. Cult. Herit.* **2010**, *11*, 138–144. [[CrossRef](#)]
32. Lasorsa, C.; Pineda, R.; Woloj, S.; Versaci, R. Silicon Carbide Coating obtained by Plasma Enhanced Chemical Vapor Deposition (PECVD) technique, properties and use in nuclear reactors. *AATN* **2014**, *128*.
33. Terpilowski, K.; Goncharuk, O. Hydrophobic properties of hexamethyldisilazane modified nanostructured silica films on glass: Effect of plasma pre-treatment of glass and polycondensation features. *Mater. Res. Express* **2018**, *5*, 016409. [[CrossRef](#)]
34. Abdulsada, A.H.; Mishjil, K.A.; Abd, A.N. Effect of thermal annealing on properties of polycrystalline Titanium dioxide (TiO₂) thin film prepared by simple chemical method. *J. Phys.* **2018**, *1032*, 012037. [[CrossRef](#)]
35. Reyes-Coronado, D.; Rodríguez-Gattorno, G.; Espinosa-Pesqueira, M.; Cab, C.; de Coss, R.D.; Oskam, G. Phase-pure TiO₂ nanoparticles: anatase, brookite and rutile. *Nanotechnology* **2008**, *19*, 145605. [[CrossRef](#)]
36. Luna, M.; Gatica, J.M.; Vidal, H.; Mosquera, M.J. One-pot synthesis of Au/N-TiO₂ photocatalysts for environmental applications: Enhancement of dyes and NO_x photodegradation. *Powder Technol.* **2019**, *355*, 793–807. [[CrossRef](#)]
37. Maness, P.C.; Smolinski, S.; Blake, D.M.; Huang, Z.; Wolfrum, E.J.; Jacoby, W.A. Bactericidal activity of photocatalytic TiO₂ reaction: Toward an understanding of its killing mechanism. *Appl. Environ. Microbiol.* **1999**, *65*, 4094–4098. [[CrossRef](#)]
38. Rodríguez-Méndez, A.; Guzmán, C.; Elizalde-Peña, E.A.; Escobar-Alarcón, L.; Vega, M.; Rivera, J.A.; Esquivel, K. Effluent disinfection of real wastewater by Ag-TiO₂ nanoparticles photocatalysis. *J. Nanosci. Nanotechnol.* **2017**, *17*, 711–719. [[CrossRef](#)]
39. Wang, L.; Wang, X.; Cui, S.; Fan, X.; Zu, B.; Wang, C. TiO₂ supported on silica nanolayers derived from vermiculite for efficient photocatalysis. *Catal. Today* **2013**, *216*, 95–103. [[CrossRef](#)]
40. Hernández, R.; Olvera-Rodríguez, I.; Guzmán, C.; Medel, A.; Escobar-Alarcón, L.; Brillas, E.; Sirés, I.; Esquivel, K. Microwave-assisted sol-gel synthesis of an Au-TiO₂ photoanode for the advanced oxidation of paracetamol as model pharmaceutical pollutant. *Electrochem. Commun.* **2018**, *96*, 42–46. [[CrossRef](#)]
41. Lee, J.; Othman, M.; Eom, Y.; Lee, T.G.; Kim, W.; Kim, J. The effects of sonification and TiO₂ deposition on the micro-characteristics of the thermally treated SiO₂/TiO₂ spherical core-shell particles for photo-catalysis of methyl orange. *Microporous Mesoporous Mater.* **2008**, *116*, 561–568. [[CrossRef](#)]
42. Hashimoto, K.; Irie, H.; Fujishima, A. TiO₂ photocatalysis: a historical overview and future prospects. *Jpn. J. Appl. Phys.* **2005**, *44*, 8269. [[CrossRef](#)]
43. Esquivel, K.; Rodríguez, F.; González, M.V.; Escobar-Alarcón, L.; Ortiz-Frade, L.; Godínez, L.A. Titanium dioxide doped with transition metals (M x Ti 1- x O 2, M: Ni, Co): Synthesis and characterization for its potential application as photoanode. *J. Nanopart. Res.* **2011**, *13*, 3313–3325. [[CrossRef](#)]
44. Castillo, R.; Koch, B.; Ruiz, P.; Delmon, B. Influence of preparation methods on the texture and structure of titania supported on silica. *J. Mater. Chem.* **1994**, *4*, 903–906. [[CrossRef](#)]
45. Ooka, C.; Yoshida, H.; Suzuki, K.; Hattori, T. Highly hydrophobic TiO₂ pillared clay for photocatalytic degradation of organic compounds in water. *Microporous Mesoporous Mater.* **2004**, *67*, 143–150. [[CrossRef](#)]
46. Al-Asbahi, B.A. Influence of anatase titania nanoparticles content on optical and structural properties of amorphous silica. *Mater. Res. Bull.* **2017**, *89*, 286–291. [[CrossRef](#)]
47. Sakohara, S.; Nishikawa, K. Compaction of TiO₂ suspension utilizing hydrophilic/hydrophobic transition of cationic thermosensitive polymers. *J. Colloid Interface Sci.* **2004**, *278*, 304–309. [[CrossRef](#)]
48. Waits, R.K. Planar magnetron sputtering. *J. Vac. Sci. Technol.* **1978**, *15*, 179–187. [[CrossRef](#)]
49. Kelly, P.J.; Arnell, R.D. Magnetron sputtering: a review of recent developments and applications. *Vacuum* **2000**, *56*, 159–172. [[CrossRef](#)]
50. Sigmund, P. Theory of sputtering. I. Sputtering yield of amorphous and polycrystalline targets. *Phys. Rev.* **1969**, *184*, 383. [[CrossRef](#)]
51. Mazur, M.; Wojcieszak, D.; Kaczmarek, D.; Domaradzki, J.; Song, S.; Gibson, D.; Placido, F.; Mazur, P.; Kalisz, M.; Poniedzialek, A. Functional photocatalytically active and scratch resistant antireflective coating based on TiO₂ and SiO₂. *Appl. Surf. Sci.* **2016**, *380*, 165–171. [[CrossRef](#)]

52. Biswas, S.; Prabakar, K.; Takahashi, T.; Nakashima, T.; Kubota, Y.; Fujishima, A. Study of photocatalytic activity of TiO₂ thin films prepared in various Ar/ O₂ ratio and sputtering gas pressure. *J. Vac. Sci. Technol. Vac. Surf. Film.* **2007**, *25*, 912–916. [[CrossRef](#)]
53. Jeong, S.H.; Kim, J.K.; Kim, B.S.; Shim, S.H.; Lee, B.T. Characterization of SiO₂ and TiO₂ films prepared using rf magnetron sputtering and their application to anti-reflection coating. *Vacuum* **2004**, *76*, 507–515. [[CrossRef](#)]
54. Morales, A.M.; Lieber, C.M. A laser ablation method for the synthesis of crystalline semiconductor nanowires. *Science* **1998**, *279*, 208–211. [[CrossRef](#)]
55. Nolte, S.; Momma, C.; Jacobs, H.; Tünnermann, A.; Chichkov, B.N.; Wellegehausen, B.; Welling, H. Ablation of metals by ultrashort laser pulses. *JOSA B* **1997**, *14*, 2716–2722. [[CrossRef](#)]
56. Ravi-Kumar, S.; Lies, B.; Zhang, X.; Lyu, H.; Qin, H. Laser ablation of polymers: A review. *Polym. Int.* **2019**, *68*, 1391–1401. [[CrossRef](#)]
57. Barberio, M.; Veltri, S.; Imbrogno, A.; Stranges, F.; Bonanno, A.; Antici, P. TiO₂ and SiO₂ nanoparticles film for cultural heritage: Conservation and consolidation of ceramic artifacts. *Surf. Coat. Technol.* **2015**, *271*, 174–180. [[CrossRef](#)]
58. Hernández-Padrón, G.; García-Garduño, M.V. Sol-gel, one technology by produced nanohybrid with anticorrosive properties. *Phys. Procedia* **2013**, *48*, 102–108. [[CrossRef](#)]
59. Wen, J.; Mark, J.E. Sol-gel preparation of composites of poly (dimethylsiloxane) with SiO₂ and SiO₂/TiO₂, and their mechanical properties. *Polym. J.* **1995**, *27*, 492. [[CrossRef](#)]
60. Zhang, W.; Tu, J.; Long, W.; Lai, W.; Sheng, Y.; Guo, T. Preparation of SiO₂ anti-reflection coatings by sol-gel method. *Energy Procedia* **2017**, *130*, 72–76. [[CrossRef](#)]
61. Son, S.; Hwang, S.H.; Kim, C.; Yun, J.Y.; Jang, J. Designed synthesis of SiO₂/TiO₂ core/shell structure as light scattering material for highly efficient dye-sensitized solar cells. *ACS Appl. Mater. Interfaces* **2013**, *5*, 4815–4820. [[CrossRef](#)]
62. Budiarti, H.A.; Puspitasari, R.N.; Hatta, A.M.; Risanti, D.D. Synthesis and Characterization of TiO₂@ SiO₂ and SiO₂@ TiO₂ Core-Shell Structure Using Lapindo Mud Extract via Sol-Gel Method. *Procedia Eng.* **2017**, *170*, 65–71. [[CrossRef](#)]
63. Lee, J.W.; Kong, S.; Kim, W.S.; Kim, J. Preparation and characterization of SiO₂/TiO₂ core-shell particles with controlled shell thickness. *Mater. Chem. Phys.* **2007**, *106*, 39–44. [[CrossRef](#)]
64. Ang, T.P.; Toh, C.S.; Han, Y.F. Synthesis, characterization, and activity of visible-light-driven nitrogen-doped TiO₂- SiO₂ mixed oxide photocatalysts. *J. Phys. Chem.* **2009**, *113*, 10560–10567.
65. Kim, C.; Choi, M.; Jang, J. Nitrogen-doped SiO₂/TiO₂ core/shell nanoparticles as highly efficient visible light photocatalyst. *Catal. Commun.* **2010**, *11*, 378–382. [[CrossRef](#)]
66. Deng, Z.Y.; Wang, W.; Mao, L.H.; Wang, C.F.; Chen, S. Versatile superhydrophobic and photocatalytic films generated from TiO₂-SiO₂@ PDMS and their applications on fabrics. *J. Mater. Chem.* **2014**, *2*, 4178–4184. [[CrossRef](#)]
67. Kitsou, I.; Panagopoulos, P.; Maggos, T.; Arkas, M.; Tsetsekou, A. Development of SiO₂@ TiO₂ core-shell nanospheres for catalytic applications. *Appl. Surf. Sci.* **2018**, *441*, 223–231. [[CrossRef](#)]
68. Kapridaki, C.; Maravelaki-Kalaitzaki, P. TiO₂-SiO₂-PDMS nano-composite hydrophobic coating with self-cleaning properties for marble protection. *Prog. Org. Coat.* **2013**, *76*, 400–410. [[CrossRef](#)]
69. Kapridaki, C.; Pinho, L.; Mosquera, M.J.; Maravelaki-Kalaitzaki, P. Producing photoactive, transparent and hydrophobic SiO₂-crystalline TiO₂ nanocomposites at ambient conditions with application as self-cleaning coatings. *Appl. Catal. Environ.* **2014**, *156*, 416–427. [[CrossRef](#)]
70. Sinkó, K. Influence of chemical conditions on the nanoporous structure of silicate aerogels. *Materials* **2010**, *3*, 704–740. [[CrossRef](#)]
71. Lupacchini, M.; Mascitti, A.; Giachi, G.; Tonucci, L.; d’Alessandro, N.; Martinez, J.; Colacino, E. Sonochemistry in non-conventional, green solvents or solvent-free reactions. *Tetrahedron* **2017**, *73*, 609–653. [[CrossRef](#)]
72. Wood, R.J.; Lee, J.; Bussemaker, M.J. A parametric review of sonochemistry: control and augmentation of sonochemical activity in aqueous solutions. *Ultrason. Sonochem.* **2017**, *38*, 351–370. [[CrossRef](#)] [[PubMed](#)]
73. Chatel, G. How sonochemistry contributes to green chemistry? *Ultrason. Sonochem.* **2018**, *40*, 117–122. [[CrossRef](#)] [[PubMed](#)]

74. Mettin, R.; Cairós, C.; Troia, A. Sonochemistry and bubble dynamics. *Ultrason. Sonochem.* **2015**, *25*, 24–30. [[CrossRef](#)] [[PubMed](#)]
75. Pokhrel, N.; Vabbina, P.K.; Pala, N. Sonochemistry: science and engineering. *Ultrason. Sonochem.* **2016**, *29*, 104–128. [[CrossRef](#)]
76. Rosales, A.; Maury-Ramírez, A.; Gutiérrez, R.; Guzmán, C.; Esquivel, K. SiO₂@ TiO₂ coating: synthesis, physical characterization and photocatalytic evaluation. *Coatings* **2018**, *8*, 120. [[CrossRef](#)]
77. Xu, Q.T.; Li, J.C.; Xue, H.G.; Guo, S.P. Binary iron sulfides as anode materials for rechargeable batteries: Crystal structures, syntheses, and electrochemical performance. *J. Power Sour.* **2018**, *379*, 41–52. [[CrossRef](#)]
78. Grover, I.S.; Prajapat, R.C.; Singh, S.; Pal, B. SiO₂-coated pure anatase TiO₂ catalysts for enhanced photo-oxidation of naphthalene and anthracene. *Particuology* **2017**, *34*, 156–161. [[CrossRef](#)]
79. Zhang, H.; Wang, G.; Sun, G.; Xu, F.; Li, H.; Li, S.; Fu, S. Facile synthesis of SiO₂@ TiO₂ hybrid NPs with improved photocatalytic performance. *Micro Nano Lett.* **2018**, *13*, 666–668. [[CrossRef](#)]
80. Narula, C.K.; Varshney, A.; Riaz, U. Atmospheric pressure chemical vapor deposition of SiO₂-TiO₂ antireflective films from [tri-(tert-butoxy) siloxy-tri-(tert-butoxy)] titanium,[tC₄H₉O] ₃Si-O-Ti [OtC₄H₉] ₃, which is a single source alkoxide precursor. *Chem. Vap. Depos.* **1996**, *2*, 13–15. [[CrossRef](#)]
81. Lee, S.M.; Park, J.H.; Hong, K.S.; Cho, W.J.; Kim, D.L. The deposition behavior of SiO₂-TiO₂ thin film by metalorganic chemical vapor deposition method. *J. Vac. Sci. Technol. Vac. Surf. Film.* **2000**, *18*, 2384–2388. [[CrossRef](#)]
82. Iravani, S.; Korbekandi, H.; Mirmohammadi, S.V.; Zolfaghari, B. Synthesis of silver nanoparticles: Chemical, physical and biological methods. *Res. Pharm. Sci.* **2014**, *9*, 385. [[PubMed](#)]
83. Chen, Q.; Miyaji, F.; Kokubo, T.; Nakamura, T. Apatite formation on PDMS-modified CaO-SiO₂-TiO₂ hybrids prepared by sol-gel process. *Biomaterials* **1999**, *20*, 1127–1132. [[CrossRef](#)]
84. Joshi, P.; Romero, H.; Neal, A.; Toutam, V.; Tadigadapa, S. Intrinsic doping and gate hysteresis in graphene field effect devices fabricated on SiO₂ substrates. *J. Physics Condens. Matter* **2010**, *22*, 334214. [[CrossRef](#)]
85. Ehara, T.; Machida, S. The effect of nitrogen doping on the structure of cluster or microcrystalline silicon embedded in thin SiO₂ films. *Thin Solid Films* **1999**, *346*, 275–279. [[CrossRef](#)]
86. Li, X.; He, J. Synthesis of raspberry-like SiO₂-TiO₂ nanoparticles toward antireflective and self-cleaning coatings. *ACS Appl. Mater. Interfaces* **2013**, *5*, 5282–5290. [[CrossRef](#)]
87. Wu, J.; Wang, H.; Bao, L.; Zhong, J.; Chen, R.; Sun, L. Novel raspberry-like hollow SiO₂@TiO₂ nanocomposites with improved photocatalytic self-cleaning properties: Towards antireflective coatings. *Thin Solid Films* **2018**, *651*, 48–55. [[CrossRef](#)]
88. Wilhelm, P.; Stephan, D. Photodegradation of rhodamine B in aqueous solution via SiO₂@ TiO₂ nano-spheres. *J. Photochem. Photobiol. Chem.* **2007**, *185*, 19–25. [[CrossRef](#)]
89. Wang, D.; Hou, P.; Zhang, L.; Xie, N.; Yang, P.; Cheng, X. Photocatalytic activities and chemically-bonded mechanism of SiO₂@TiO₂ nanocomposites coated cement-based materials. *Mater. Res. Bull.* **2018**, *102*, 262–268. [[CrossRef](#)]
90. Kesmez, Ö.; Çamurlu, H.E.; Burunkaya, E.; Arpaç, E. Sol-gel preparation and characterization of anti-reflective and self-cleaning SiO₂-TiO₂ double-layer nanometric films. *Sol. Energy Mater. Sol. Cells* **2009**, *93*, 1833–1839. [[CrossRef](#)]
91. Zhang, X.; Fujishima, A.; Jin, M.; Emeline, A.V.; Murakami, T. Double-layered TiO₂- SiO₂ nanostructured films with self-cleaning and antireflective properties. *J. Phys. Chem.* **2006**, *110*, 25142–25148. [[CrossRef](#)]
92. Miao, L.; Su, L.F.; Tanemura, S.; Fisher, C.A.; Zhao, L.L.; Liang, Q.; Xu, G. Cost-effective nanoporous SiO₂-TiO₂ coatings on glass substrates with antireflective and self-cleaning properties. *Appl. Energy* **2013**, *112*, 1198–1205. [[CrossRef](#)]
93. Ye, L.; Zhang, Y.; Zhang, X.; Hu, T.; Ji, R.; Ding, B.; Jiang, B. Sol-gel preparation of SiO₂/TiO₂/SiO₂-TiO₂ broadband antireflective coating for solar cell cover glass. *Sol. Energy Mater. Sol. Cells* **2013**, *111*, 160–164. [[CrossRef](#)]
94. Tricoli, A.; Righettoni, M.; Pratsinis, S.E. Anti-fogging nanofibrous SiO₂ and nanostructured SiO₂- TiO₂ films made by rapid flame deposition and in situ annealing. *Langmuir* **2009**, *25*, 12578–12584. [[CrossRef](#)]
95. Miyauchi, M.; Shimohigoshi, M.; Hashimoto, K. Hydrophilic Layered SiO₂/TiO₂/WO₃ Thin Film for Indoor Anti-Fogging Coatings. *J. Ceram. Soc. Jpn.* **2004**, *112*, S1414–S1418.
96. Eshaghi, A.; Aghaei, A.A.; Zabolian, H.; Jannesari, M.; Firoozifar, A. Transparent superhydrophilic SiO₂/TiO₂/SiO₂ tri-layer nanostructured antifogging thin film. *Ceram-Silikaty* **2013**, *57*, 210–214.

97. Tang, X.; Feng, Q.; Liu, K.; Tan, Y. Synthesis and characterization of a novel nanofibrous TiO₂/SiO₂ composite with enhanced photocatalytic activity. *Mater. Lett.* **2016**, *183*, 175–178. [[CrossRef](#)]
98. Liu, Z.; Miao, Y.E.; Liu, M.; Ding, Q.; Tjiu, W.W.; Cui, X.; Liu, T. Flexible polyaniline-coated TiO₂/SiO₂ nanofiber membranes with enhanced visible-light photocatalytic degradation performance. *J. Colloid Interface Sci.* **2014**, *424*, 49–55. [[CrossRef](#)]
99. Wu, L.; Yan, H.; Xiao, J.; Li, X.; Wang, X. Characterization and photocatalytic properties of SiO₂-TiO₂ nanocomposites prepared through gaseous detonation method. *Ceram. Int.* **2017**, *43*, 9377–9381. [[CrossRef](#)]
100. Resende, S.; Nunes, E.; Houmard, M.; Vasconcelos, W. Simple sol-gel process to obtain silica-coated anatase particles with enhanced TiO₂-SiO₂ interfacial area. *J. Colloid Interface Sci.* **2014**, *433*, 211–217. [[CrossRef](#)]
101. Dong, W.; Sun, Y.; Ma, Q.; Zhu, L.; Hua, W.; Lu, X.; Zhuang, G.; Zhang, S.; Guo, Z.; Zhao, D. Excellent photocatalytic degradation activities of ordered mesoporous anatase TiO₂-SiO₂ nanocomposites to various organic contaminants. *J. Hazard. Mater.* **2012**, *229*, 307–320. [[CrossRef](#)]
102. Duraibabu, D.; Ganeshbabu, T.; Manjumeena, R.; Dasan, P. Unique coating formulation for corrosion and microbial prevention of mild steel. *Prog. Org. Coat.* **2014**, *77*, 657–664. [[CrossRef](#)]
103. Yuranova, T.; Mosteo, R.; Bandara, J.; Laub, D.; Kiwi, J. Self-cleaning cotton textiles surfaces modified by photoactive SiO₂/TiO₂ coating. *J. Mol. Catal. Chem.* **2006**, *244*, 160–167. [[CrossRef](#)]
104. Fakin, D.; Veronovski, N.; Ojstršek, A.; Božič, M. Synthesis of TiO₂-SiO₂ colloid and its performance in reactive dyeing of cotton fabrics. *Carbohydr. Polym.* **2012**, *88*, 992–1001. [[CrossRef](#)]
105. Veronovski, N.; Sfiligoj-Smole, M.; Viota, J. Characterization of TiO₂/TiO₂-SiO₂ coated cellulose textiles. *Text. Res. J.* **2010**, *80*, 55–62. [[CrossRef](#)]
106. Pakdel, E.; Daoud, W.A.; Wang, X. Self-cleaning and superhydrophilic wool by TiO₂/SiO₂ nanocomposite. *Appl. Surf. Sci.* **2013**, *275*, 397–402. [[CrossRef](#)]
107. Pakdel, E.; Daoud, W.A. Self-cleaning cotton functionalized with TiO₂/SiO₂: Focus on the role of silica. *J. Colloid Interface Sci.* **2013**, *401*, 1–7. [[CrossRef](#)]
108. Xu, B.; Ding, J.; Feng, L.; Ding, Y.; Ge, F.; Cai, Z. Self-cleaning cotton fabrics via combination of photocatalytic TiO₂ and superhydrophobic SiO₂. *Surf. Coat. Technol.* **2015**, *262*, 70–76. [[CrossRef](#)]
109. Landi, S., Jr.; Carneiro, J.; Ferdov, S.; Fonseca, A.M.; Neves, I.C.; Ferreira, M.; Parpot, P.; Soares, O.S.; Pereira, M.F. Photocatalytic degradation of Rhodamine B dye by cotton textile coated with SiO₂-TiO₂ and SiO₂-TiO₂-HY composites. *J. Photochem. Photobiol. Chem.* **2017**, *346*, 60–69. [[CrossRef](#)]
110. Mendoza, C.; Valle, A.; Castellote, M.; Bahamonde, A.; Faraldos, M. TiO₂ and TiO₂-SiO₂ coated cement: Comparison of mechanic and photocatalytic properties. *Appl. Catal. Environ.* **2015**, *178*, 155–164. [[CrossRef](#)]
111. Pan, F.; Zhang, B.; Cai, W. The effect of hydrophilicity/hydrophobicity of TiO₂-SiO₂ composite aerogels in the epoxidation reaction. *Catal. Commun.* **2017**, *98*, 121–125. [[CrossRef](#)]
112. Dey, T.; Naughton, D. Cleaning and anti-reflective (AR) hydrophobic coating of glass surface: A review from materials science perspective. *J. Sol. Gel Sci. Technol.* **2016**, *77*, 1–27. [[CrossRef](#)]

